Preparation of Silica and Alumina Single Oxides from Commercial Preformed Sols

Steven J. Monaco and Edmond I. Ko*

Department of Chemical Engineering, Carnegie Mellon University, Pittsburgh, Pennsylvania 15213-3890

Received April 30, 1997. Revised Manuscript Received August 4, 1997[⊗]

High surface area silica and alumina powders were prepared from four commercially available colloidal silicas (Nyacol 830, 2040, 9950, and 2034DI) and three colloidal aluminas (Dispal 23N4−20, 18N4−20, and 11N7−12). Particle size distributions of the sols were obtained from dynamic light-scattering experiments and found to deviate significantly from the nominal sizes reported by the manufacturer. The sols were gelled via several methods, dried, and calcined at 773 K and above. A spherical particle packing model based on the measured sol particle size distributions was found to account for important textural properties such as surface area and pore volume of the calcined silica powders. For the calcined alumina powders, a better predictor for the textural properties was the crystallites whose aggregates form the precursor alumina sol. Nitrogen adsorption, diffuse reflectance infrared Fourier transform (DRIFT) spectroscopy, and X-ray diffraction studies of the calcined silica and alumina powders were used to characterize their structural features and transformations, hydroxyl populations, and acidic properties as a function of heat-treatment temperature. We show that the properties of metal oxides prepared from commercially available sols can be understood when such a systematic approach is taken, despite the inherent complexity of using nonmodel precursors.

Introduction

Sol−gel processing has been used to provide control over microscopic properties such as molecular structure in structural, optical, and electronic glasses and ceramics. However, despite recent efforts, the use of sol−gel methods to prepare materials of catalytic interest is not yet as mature as that of glasses and ceramics.[1,2] Control over those microscopic properties which are important in catalysis—thermal and hydrothermal stability, pore structure, etc.—has thus been less extensively explored. Of the research that has been done into the sol−gel preparation of such materials, the vast majority has involved the use of metal alkoxides as precursors to the final calcined metal oxide. In an alkoxide-based preparation, the alkoxide is first partially hydrolyzed to form a sol, which subsequently condenses into a three-dimensional polymeric network, e.g., a gel. Because the hydrolysis and condensation reactions are performed simultaneously in such an approach, it is difficult to isolate any effect of sol size on the properties of the final gel. In general, from a research perspective, the study of metal alkoxide-derived gels is desirable because alkoxides can be obtained in high purity and their solution chemistry is fairly well understood, especially with such materials as silica. However, the use of metal alkoxides as a precursor for a commercial catalyst is difficult because of their high reactivity which would lead to practical scaleup problems. Their high costs can also be a barrier, but this is mitigated by the fact that catalyst costs are often minor when compared to the market value of the final product. These reasons all justify research into the use of preformed sols instead of alkoxides to prepare catalytic materials.

The term "preformed sol" refers to the use of a precursor sol that has well-defined and stable properties and is distinct from a sol formed in situ during the gelation of an alkoxide, where the effects of the sol properties on the final gel are relatively difficult to isolate. The use of well-characterized preformed sols as a precursor to the final oxide offers a different molecular building block, i.e., a particle of colloidal size, which allows the isolation of the formation of the sol from the formation of the gel. A very powerful concept emerges: that by accessing a continuum of building block sizes, from a monomeric alkoxide precursor up through sol particles of several hundred nanometers, new nanostructured materials with unique properties can be developed. In addition, comparisons between materials prepared at different points along this continuum may allow insight into sintering mechanisms, the generation of acidity, or other properties of catalytic interest. The feasibility of such an approach has been demonstrated by Ramsay and Booth with silica and ceria[3] and Ramsay and Avery with silica, alumina, and titania.[4] More recent demonstrations include Ward and Ko with zirconia sols,[5] and Murrell and Tauster with alumina sols and mixed sols of zirconia and ceria.[6] A preformed sol preparation can lead to properties very different than those resulting from a corresponding

* To whom correspondence should be addressed.
[⊗] Abstract published in *Advance ACS Abstracts,* September 15, 1997.
(1) Ward, D. A.; Ko, E. I. *I&EC Res.* **1995**, *34*, 421.
(2) Cauqui, M. A.; Rodríguez-Izquierdo, J. M. *J. Non-Cryst. Solids* **1992**, *147/148*, 724.
(3) Ramsay, J. D. F.; Booth, B. O. *J. Chem. Soc., Faraday Trans. 1* **1983**, *79*, 173.
(4) Ramsay, J. D. F.; Avery, R. G. *Br. Ceram. Proc.* **1986**, *38*, 275.
(5) Ward, D. A.; Ko, E. I. *Langmuir* **1995**, *11*, 369.
(6) Murrell, L. L.; Tauster, S. J. In *Catalysis and Automotive Pollution Control II*; Crucq, A., Ed.; Elsevier Science: Amsterdam, 1991; p 547.

S0897-4756(97)00271-8 CCC: $14.00

alkoxide-based approach. For example, samples prepared from zirconia sols have different pore characteristics and crystallization behavior when compared to a zirconia aerogel.[5] Aside from these few examples, fundamental work on preformed sols remains scarce in the catalytic literature. In particular, there is a lack of systematic studies where a matrix of sol precursors with well-defined size distributions are compared to the structure of the oxide phases after gelation and subsequent heat treatment.[7] A basic understanding of the gelation of preformed sols, especially in relation to the subsequent structural evolution of the gels, is essential for their commercial catalytic applications. Using preformed sols to prepare oxides of catalytic interest thus offers a link between fundamental understanding and industrial relevance. This work represents an important step in providing systematic data for commercial preformed sols to both academic and industrial researchers.

In this study we have examined the properties of single oxide gels made from commercially available aqueous silica and alumina sol precursors. In general, we have taken a more systematic approach and used a wider range of sols than in the studies mentioned previously. Silica was chosen because its chemistry is well understood and because of its wide range of applications from biology to photography.[8] Alumina is also an industrially important material, used for such purposes as a catalyst support or in washcoats on monolith structures.[9] Since we are interested in these materials for catalytic applications, we have focused on defining the pore characteristics and acidic properties of our samples. We have also characterized the hydroxyl groups because of their importance in sintering[10,11] and their role as anchoring sites for the surface grafting of another oxide.[12,13] In the future, we will prepare alumina−silica mixed oxide gels from these sols and attempt to explain both their textural (surface area and pore volume) and chemical (acidity) properties using the knowledge gained from this study of single oxide gels.

Experimental Section

Sample Preparation. Four colloidal silicas, provided by Eka Nobel, Inc., were used: Nyacol grades 830, 2040, 2034DI, and 9950. Nyacol grade 2034DI is an acid-stable colloidal silica, while the remainder are base-stable colloidal silicas. Four colloidal aluminas, provided by Vista Chemical Co., were used: Dispal 11N7−12, 18N4−20, and 23N4−20. Dispal 18N4−20 and 23N4−20 are acid-stable colloidal aluminas, while 11N7−12 is stabilized at neutral pH. The Dispal aluminas are manufactured through a proprietary alkoxide process which produces boehmite (γ-AlOOH) crystallite particles.[14] Tables 1 and 2 respectively list the manufacturer's specifications for the silica and alumina sols.

Table 1. Colloidal Silicas Available from Eka Nobel, Inc.[a]

Nyacol grade	830	2040	9950	2034DI
particle size, nm	8	20	100	20
SiO_2, wt %	30	40	50	34
Na_2O, wt %	0.55	0.38	0.15	
pH	10.5	10	9.3	3.0

[a] Data furnished by manufacturer.

Table 2. Colloidal Aluminas Available from Vista Chemical Co.[a]

Dispal grade	11N7−12	18N4−20	23N4−20
particle size, nm	415	94	90
Al_2O_3, wt %	12	20	20
NO_3^-, wt %	0.02	0.29	0.38
pH	6.5−7.2	3.7−3.9	4.3−4.7
crystallite size (020), nm	20.4	7.8	5.6
crystallite size (120), nm	38.4	15.1	10.3

[a] Data furnished by manufacturer.

Three main preparative variables were examined: the initial sol particle size, the concentration of SiO_2 or Al_2O_3 in the total gel mixture, and the concentration of HNO_3 in the total gel mixture. The initial sol size was controlled by changing sol precursors. The metal oxide and acid concentrations were controlled by varying the amounts of nitric acid and/or water which were added to the sol precursor. The majority of the powders prepared were gelled by the addition of nitric acid (HNO_3) [Fisher] or by drying the sol (diluted in some cases) in a vacuum oven without first forming a gel. For the silicas, this nitric acid addition resulted in a pH < 1 in the wet gels. The colloidal alumina could be gelled with a much smaller amount of acid addition, resulting in a correspondingly smaller pH change. Colloidal suspensions can be destabilized with acids to form gels through a hydroxyl group condensation mechanism catalyzed by H^+ and the collapse of the repulsive double layer.[8,15,16] Trace fluoride ions may also be a factor in the gelation of aqueous silica sols.[8,16]

In addition, the effects on textural properties of two additional preparation techniques were investigated using silica sols. The first, used with the Nyacol 830 and 2034DI silica sols, was the addition of 1-propanol (C_3H_7OH) [Fisher] to a sol first neutralized to pH 7 with nitric acid (Nyacol 830) or ammonium hydroxide (Nyacol 2034DI). This method, suggested by Iler,[8] is supposed to form a gel with minimal points of contact between the particles and thus might be expected to have the highest surface area of the techniques studied. The final technique, used with the Nyacol 830 silica sol, was to first form the gel using the low-pH technique, adding an equal volume of ethanol (C_2H_7OH) [Fisher] to the gel, and then vacuum filtering this mixture. This solvent exchange procedure was performed twice on the gel to remove as much of the water present in the gel as possible. This procedure was designed to create a strong gel by promoting strong interparticle bonds while at the same time lowering the capillary forces during drying. The use of the Nyacol 2040 and 2034DI silica precursors allowed the investigation of the effects of using basic and acidic precursors at the same nominal 20 nm sol particle size. Table 3 summarizes the preparative parameters used and the sample nomenclature for the 12 silica powders that were prepared.

As previously mentioned, alumina gels were prepared by the addition of HNO_3 or by simply drying the sols in a vacuum oven. One additional gel was prepared by the addition of NH_4OH [Fisher] to Dispal 23N4−20. Murrell and Tauster studied alumina sols gelled at pH 9 with NH_4OH,[6] but in our case the amount of base added was much smaller, resulting in the gel still being formed under acidic conditions. Table 4 summarizes the preparative parameters used and the sample nomenclature for the nine alumina powders that were prepared.

(7) Murrell, L. L. *Catal. Today* **1997**, *35*, 225.
(8) Iler, R. K. *The Chemistry of Silica*; John Wiley & Sons: New York, 1979.
(9) Murrell, L. L.; Tauster, S. J.; Anderson, D. R. In *New Frontiers in Catalysis*; Guczi, L., Solymosi, F., Tetenyl, P., Eds.; Elsevier Science: Amsterdam, 1993; p 681.
(10) Burtin, P.; Brunelle, J. P.; Pijolat, M.; Soustelle, M. *Appl. Catal.* **1987**, *34*, 239.
(11) Beguin, B.; Garbowki, E.; Primet, M. *J. Catal.* **1991**, *127*, 595.
(12) Wachs, I. E. *Catal. Today* **1996**, *27*, 437.
(13) Mastikhin, V. M.; Nosov, A. V.; Terskikh, V. V.; Zamaraev, K. I.; Wachs, I. E. *J. Phys. Chem.* **1994**, *98*, 13621.
(14) Vista Chemical Co. Dispersible Aluminas product literature.
(15) Brinker, C. J.; Scherer, G. W. *Sol−Gel Science*; Academic Press: New York, 1990.
(16) Iler, R. K. *J. Phys. Chem.* **1952**, *56*, 680.

Table 3. Silica Gels: Nomenclature and Preparative Parameters

sample name[a]	Nyacol precursor	SiO_2 conc (M)	HNO_3 conc (M)	NH_4OH conc (M)	1-PrOH conc (M)	gel time (s)
8 SiO_2−(3.0/0.08/P)	830	3.0	0.08	0.0	6.6	n/a[b]
8 SiO_2−(6.1/0.0)	830	6.1	0.0	0.0	0.0	n/a[b]
8 SiO_2−(3.5/6.5/E)	830	3.5	6.5	0.0	0.0	43
8 SiO_2−(3.5/6.5)	830	3.5	6.5	0.0	0.0	55
20 SiO_2−(3.5/6.5)	2040	3.5	6.5	0.0	0.0	240
20 SiO_2−(3.5/4.5)	2040	3.5	4.5	0.0	0.0	2782
20 SiO_2−(2.5/6.5)	2040	2.5	6.5	0.0	0.0	677
20 SiO_2−(2.5/4.5)	2040	2.5	4.5	0.0	0.0	7736
20A SiO_2−(3.5/0.02B/P)	2034DI	3.5	0.0	0.02	6.7	270
20A SiO_2−(3.5/6.5)	2034DI	3.5	6.5	0.0	0.0	233
20A SiO_2−(3.5/4.5)	2034DI	3.5	4.5	0.0	0.0	2771
100 SiO_2−(3.5/6.5)	9950	3.5	6.5	0.0	0.0	>900

[a] Nomenclature is *xx* SiO_2−(*yy*/*zz*/*a*) where *xx* = nominal sol particle size in nm (A indicates acid stable sol), *yy* = SiO_2 molar concentration in wet gel, *zz* = HNO_3 or NH_4OH molar concentration in wet gel (B denotes base addition), and *a* = P for 1-PrOH or E for ethanol. [b] Not applicable.

Table 4. Alumina Gels: Nomenclature and Preparative Parameters

sample name[a]	Dispal precursor	Al_2O_3 conc (M)	HNO_3 conc (M)	NH_4OH conc (M)	gel time (s)
90 Al_2O_3−(1.0/0.0)	23N4−20	1.0	0.0	0.0	n/a[b]
90 Al_2O_3−(2.33/0.0)	23N4−20	2.33	0.0	0.0	n/a[b]
90 Al_2O_3−(1.0/0.033B)	23N4−20	1.0	0.0	0.033	<10
90 Al_2O_3−(1.0/0.14)	23N4−20	1.0	0.14	0.0	395
90 Al_2O_3−(1.0/0.18)	23N4−20	1.0	0.18	0.0	<10
94 Al_2O_3−(1.0/0.0)	18N4−20	1.0	0.0	0.0	n/a[b]
94 Al_2O_3−(1.0/0.14)	18N4−20	1.0	0.14	0.0	128
94 Al_2O_3−(1.5/0.14)	18N4−20	1.5	0.14	0.0	138
415 Al_2O_3−(1.0/0.0)	11N7−12	1.0	0.0	0.0	n/a[b]

[a] Nomenclature is *xx* Al_2O_3−(*yy*/*zz*) where *xx* = nominal sol particle size in nm, *yy* = Al_2O_3 molar concentration in wet gel, *zz* = HNO_3 or NH_4OH molar concentration in wet gel (B denotes base addition). [b] Not applicable.

For the silica or alumina powders prepared with nitric acid or ammonium hydroxide, the desired amount of acid or base was diluted in the required amount of distilled water in a 50 or 100 mL beaker (depending on the volume required) with a magnetic stir bar. To have a well-mixed suspension, the precursor sol containers were shaken before measuring out 15 mL into a separate 50 or 100 mL beaker, depending on the projected total volume of sol and acid/base plus water. It was found that this agitation of the container was necessary for reproducible results during a prior study of zirconia sols.[5] The precursor sol was also stirred with a magnetic stir bar. The acid or base solution was then added to the precursor over about 5 s. Stirring was continued until the vortex created by the stirbar disappeared. This time was defined as the gel time. The pH of the silica sols after the addition of the nitric acid/water was reduced to less than 1, while the pH of the alumina sols was changed by less than one pH unit with either acid or base addition. The gelation behavior of all of the silica powders prepared with this technique were similar, with higher acid and/or silica concentrations giving faster gel times. The silica gels were typically opaque white, with the Nyacol 830 based gels giving a more translucent gel. The gel time for the alumina gels was a strong function of the acid concentration, with higher acid concentrations giving faster gel times. The effect on gel time of concentration was negligible for the pair of powders prepared at different alumina concentrations—the 10 s difference in gel times is within the precision of times achievable with repeated experiments. The alumina gel formed with ammonium hydroxide gelled immediately upon addition of the base. The alumina gels were slightly translucent upon formation. Both the silica and alumina gels were very weak upon formation and would firm up somewhat while aging, but could be stirred with a spatula fairly easily after aging for 3 h. Even after aging, the wet alumina gels as a whole were more easily sheared than the silica gels. The gels were dried in an oven at 383 K after a 3 h aging period.

For the two silica gels formed with 1-propanol, 15 mL of the precursor sol was measured into a 100 mL beaker with a magnetic stir bar. Concentrated nitric acid was added to the sol to adjust its pH to 7. After allowing the solution to stir for 10 min, 15 mL of 1-propanol was added. The Nyacol 830 immediately formed a gel, while the Nyacol 2034DI took 4.5 min to form. These gels were allowed to air-dry for 1 day, forming a hard white disk of silica. This disk was broken up with a metal spatula before being dried in an oven at 383 K.

The ethanol-washed silica gel was first prepared with nitric acid using the same procedure used for the low pH silica gels. After a 3 h aging period, an equal volume of ethanol was stirred into the gel. This mixture was then vacuum filtered twice, poured into a glass dish and left to dry overnight in a nitrogen-purged glovebox. The resulting powder was then dried at 383 K.

All of the samples (silica and alumina) were first dried for 3 h at 383 K. The first hour of drying was at atmospheric pressure, and the final 2 h were under vacuum at a pressure of 3.4 kPa absolute. The gels were then cooled and covered overnight. In the next heat treatment step, the gels were dried at 523 K under vacuum for an additional 3 h, cooled, and ground to a white powder of less than 100 mesh. The ground powders were calcined at 773 K for 2 h in flowing oxygen (24 L/h). Portions of the 773 K calcined powders were subsequently calcined at 1173 K for 2 h. Selected alumina and silica powders calcined at 1173 K were then calcined at 1373 K for an additional 2 h. One alumina powder [90 Al_2O_3−(1.0/0.14)] calcined at 1373 K was subsequently calcined at 1473 K in an air-purged box furnace.

Characterization. Textural properties (BET surface areas, pore volumes, and pore size distributions) of the powders were determined by nitrogen adsorption performed on a Quantachrome Corp. Autosorb-1 gas sorption system. Before analysis, powders were outgassed at 473 K (383 K for powders previously heat treated to only 383 K) for 3 h under vacuum.

Particle size distributions of both the silica (Nyacol 830, 2040, 2034DI, and 9950) and alumina (Dispal 23N4−20, 18N4−20, and 11N7−12) precursor sols were performed by Particle Sizing Systems, Inc. using a NICOMP 370 submicron particle sizer. The NICOMP 370 uses dynamic light scattering (DLS) to measure a sample's particle size distribution. The DLS technique measures the time dependence of light intensity fluctuations calculated from an autocorrelation function of the measured scattered intensity. This dependence is related to the diffusion coefficient of the particles and then to the particle size through the Stokes−Einstein equation. The autocorrelation function is a weighted sum of exponentially decaying functions, each of which corresponds to a different particle diameter. The inversion of this function, which can be difficult for complex distributions, gives the intensity-weighted particle size distributions.[17] For simple unimodal distributions, a Gaussian two-parameter fit to the raw data gives a mean diameter, standard deviation, and a baseline adjust value. A nonzero baseline adjust indicates the presence of large, off-scale particles. Large values (>3) of the Gaussian

(17) Stock, R. S.; Ray, W. H. *J. Polym. Sci., Polym. Phys. Ed.* **1985**, *23*, 1393.

Table 5. Silica Gels: Selected Data[a]

sample name	Nyacol precursor	5-pt BET surface area (m^2/g)[a]	pore vol (cm^3/g)	porosity, ϵ (%)[b]	$R_{pore,avg}$ (nm)[c]	nominal $D_{particle}$ (nm)	calculated $D_{particle}$[d] (nm)	particle coordination no., n[d]
8 SiO_2−(3.0/0.1/P)	830	152	0.56	55	7.3	8	17.0	5.1
8 SiO_2−(6.1/0.0)	830	132	0.25	36	3.9	8	19.0	8.6
8 SiO_2−(3.5/6.5/E)	830	219	0.89	66	8.1	8	11.7	4.0
8 SiO_2−(3.5/6.5)	830	192	0.73	62	7.6	8	13.4	4.4
20 SiO_2−(3.5/6.5)	2040	138	0.61	57	8.8	20	18.9	4.9
20 SiO_2−(3.5/4.5)	2040	157	0.61	58	7.8	20	14.2	4.8
20 SiO_2−(2.5/6.5)	2040	153	0.62	58	8.1	20	16.9	4.8
20 SiO_2−(2.5/4.5)	2040	145	0.60	57	8.3	20	17.9	4.9
20A SiO_2−(3.5/0.02B/P)	2034DI	157	0.45	50	5.8	20	16.3	5.8
20A SiO_2−(3.5/6.5)	2034DI	180	0.63	58	7.0	20	14.2	4.8
20A SiO_2−(3.5/4.5)	2034DI	181	0.62	58	6.8	20	14.2	4.8
100 SiO_2−(3.5/6.5)	9950	71	0.54	54	15.1	100	37.4	5.2

[a] Powders calcined at 773 K for 2 h. [b] Calculated as $\epsilon = \rho V_{pore}/[1 + \rho V_{pore}]$ where $\rho_{SiO_2} = 2.2$ g/cm^3 (see text). [c] Calculated as $R_{pore,avg} = 2V_{pore}/S_{BET}$. [d] Calculated using spherical particle packing model.

Table 6. Alumina Gels: Selected Data[a]

sample name	Nyacol precursor	5-pt BET surface area (m^2/g)[a]	pore vol (cm^3/g)	porosity, ϵ (%)[b]	$R_{pore,avg}$ (nm)[c]	nominal $D_{particle}$ (nm)	calculated $D_{particle}$[d] (nm)	particle coordination no., n[d]
90 Al_2O_3−(1.0/0.0)	23N4−20	243	0.40	56	3.3	90	6.7	5.0
90 Al_2O_3−(2.33/0.0)	23N4−20	232	0.38	55	3.3	90	7.0	5.1
90 Al_2O_3−(1.0/0.033B)	23N4−20	237	0.48	61	4.0	90	7.0	4.5
90 Al_2O_3−(1.0/0.14)	23N4−20	227	0.38	55	3.3	90	7.2	5.1
90 Al_2O_3−(1.0/0.18)	23N4−20	223	0.37	54	3.3	90	7.3	5.2
94 Al_2O_3−(1.0/0.0)	18N4−20	187	0.43	58	4.6	94	9.1	4.8
94 Al_2O_3−(1.0/0.14)	18N4−20	167	0.41	57	5.0	94	10.3	4.9
94 Al_2O_3−(1.5/0.14)	18N4−20	157	0.42	57	5.4	94	11.0	4.8
415 Al_2O_3−(1.0/0.0)	11N7−12	90	0.63	67	13.9	415	20.1	4.0

[a] Powders calcined at 773 K for 2 h. [b] Calculated as $\epsilon = \rho V_{pore}/[1 + \rho V_{pore}]$ where $\rho_{\gamma-Al_2O_3} = 3.2$ g/cm^3 (see text). [c] Calculated as $R_{pore,avg} = 2V_{pore}/S_{BET}$. [d] Calculated using spherical particle packing model.

"goodness of fit" parameter, χ^2, indicate that the particle size distribution deviates significantly from a Gaussian distribution. In these cases, the NICOMP 370 applies a LaPlace transform, least-squares fit algorithm to the raw data to determine the particle size distribution. The NICOMP analysis can, in principle, resolve uni-, bi-, and trimodal distributions and thus give the true particle size distribution when the Gaussian model is not appropriate. The Gaussian and NICOMP analysis intensity-weighted data are further processed by the NICOMP 370 to obtain both volume- and number-weighted particle size distributions.[18,19] It is important to understand the proper interpretation of DLS data and how, as we will show, the common assumption of a unimodal, Gaussian particle size distribution can lead to misleading results.

Diffuse reflectance infrared Fourier transform (DRIFT) experiments were performed using a Mattson Galaxy 5020 FTIR spectrometer with a DTGS (deuterium triglycine sulfate) detector and a Harrick Scientific Praying Mantis diffuse reflection attachment (DRA-2-MA1). Each IR spectrum was obtained by averaging 128 scans taken over a range of 400−4000 cm^{-1} with a 2 cm^{-1} resolution. Data were normalized with respect to the ∼460 cm^{-1} Si−O−Si bend frequency for the silica powders or the broad structural peak at 400−1000 cm^{-1} for the alumina powders. Both ex situ and in situ DRIFT spectra were taken using 2 wt % sample diluted in KBr. In the ex situ spectra, the hydroxyl region was obscured by physisorbed water. To remove this weakly bound water and more carefully examine the surface hydroxyl groups, samples were heated under He flow in a Harrick reaction chamber (HVC-DR2). For these in situ experiments, the samples were first scanned at ambient conditions after 10 min of 50 cm^3/min He flow. They were then heated to 473 K at 10 K/min and held there for 1 h. Scans were taken after 10 and 50 min of this 473 K step. The temperature was then reduced to 383 K at 12.5 K/min and held there for an additional hour. Scans were again taken after 10 and 50 min. The temperature was then returned to ambient and a final scan taken. This heat treatment schedule is similar to that used in the pretreatment for 1-butene isomerization testing of other catalytic oxide materials.[20]

In situ pyridine adsorption experiments were also performed using the Harrick Praying Mantis and reaction chamber apparatus. These DRIFT spectra were taken using 5 wt % sample diluted in KBr in order to enhance the pyridine signal. The samples were pretreated to 588 K under 50 cm^3/min He flow at a heating rate of ∼15−20 K/min, cooled to 373 K, and then exposed for 15 min to pyridine introduced via a bubbler. After the pyridine exposure, the samples were then heated to 713 K in a stepwise manner (373, 423, 473, 553, 623, 673, 713 K) with DRIFT spectra taken after 5 min at each step.

To determine the dependence of the crystallization of silica on temperature as well as the transition temperatures of the alumina crystalline phases, X-ray diffraction (XRD) using a Rigaku D/Max diffractometer with Cu Kα radiation was performed on selected powders.

Results and Discussion

Effect of Precursor Sol Size on Textural Properties. Tables 5 and 6 respectively list surface area, pore volume, porosity, and average pore radius data for the 12 silica powders and 9 alumina powders after calcination at 773 K for 2 h. Figure 1a shows the effect of SiO_2 sol size on the pore size distribution curves calculated from N_2 desorption data for the 3.5 M SiO_2/6.5 M HNO_3 subset of silica powders prepared at low pH, while Figure 1b shows equivalent data for the 1.0 M Al_2O_3/0.0 M HNO_3 subset of alumina powders. For the silica

(18) Kourti, T.; MacGregor, J. F.; Hamielec, A. E.; Nicoli, D. F.; Elings, V. B. In *Polymer Characterization*; Craver, C. D., Provder, T., Eds.; American Chemical Society: Washington, DC, 1990.

(19) Particle Sizing Systems, NICOMP 370 Submicron Particle Sizer product literature.

(20) Miller, J. B.; Ko, E. I. *J. Catal.* **1996**, *159*, 58.

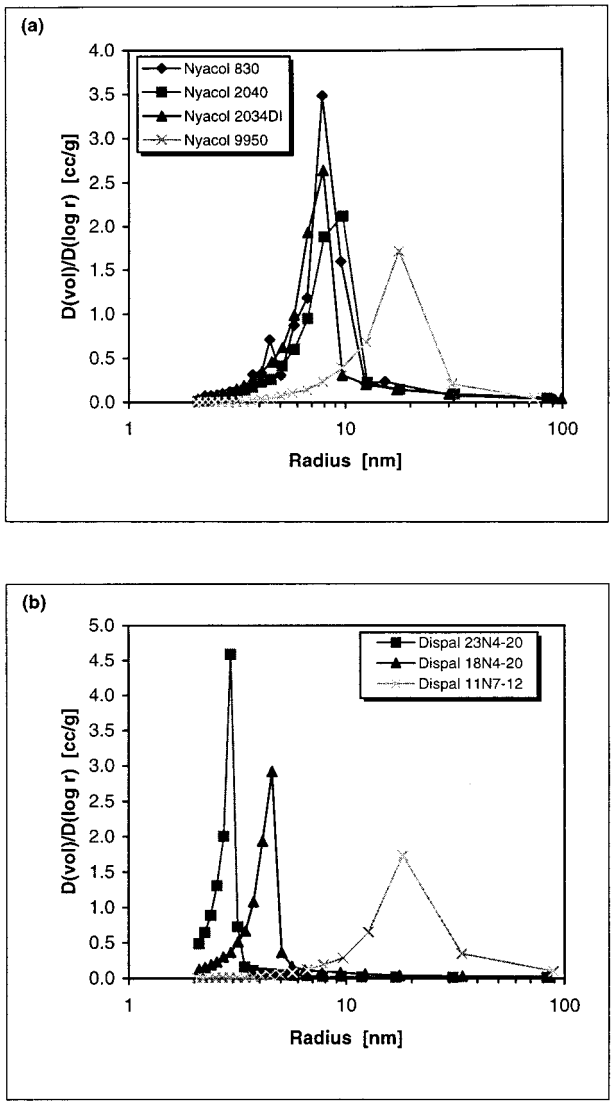

Figure 1. Effect of sol size on the pore size distribution of (a) silica powders and (b) alumina powders. Silica gels prepared at low pH with composition of 3.5 M SiO_2 and 6.5 M HNO_3. Alumina gels diluted to 1.0 M Al_2O_3 and dried. All powders calcined at 773 K for 2 h. Data derived from desorption isotherm.

powders, increasing sol size leads to a corresponding shift upward in the average pore diameter for the powders prepared from the base-stable sols (Nyacol 830, 2040, and 9950). Note, however, that the powder made from the acid-stable Nyacol 2034DI behaves more like the Nyacol 830 than the Nyacol 2040 even though their nominal particle sizes are the same. Increasing sol size leads to a corresponding shift upward in the average pore diameter for the alumina powders as well, along with a corresponding broadening of the distributions. For both the silica and alumina powders, the nominal particle size supplied by the manufacturer is larger than the average pore diameters. For nonporous particles, the pore diameters should be on the order of the particle size,[8,21] and, if the sol particles remain relatively intact after gelation, one of two conclusions can be made: either the nominal particle sizes are incorrect, or the sol particles are porous. If the sol particles do not remain intact during gelation, this pore diameter–particle size relationship does not hold. As we shall see, the nominal particle sizes for both the silica and alumina sols are inaccurate, and there is evidence that the alumina sol particles do not remain intact upon gelation. It is the crystallites that make up the alumina sol particles that can be considered to be the true primary particles in an alumina gel.

In an attempt to verify the manufacturer's nominal particle sizes, a spherical particle packing model[8,21] was applied using the measured textural properties of the powders shown in Tables 5 and 6. The particle packing model, applied by Ramsay and Avery to the packing of spherical particles under compression, assumes that the primary particles in a dried gel are nonporous spheres.[21] For our calculations, these spheres were assumed to have either the density of amorphous silica, 2.2 g/cm^3,[8] or that of γ-alumina, 3.2 g/cm^3.[22] This model of a gel network assumes that the oxide exists as colloidally sized "marbles" of a fixed size connected to some number of other "marbles" by the interparticle bonds. S_G, the specific surface area of the unaggregated spheres or the total geometrical surface area, is given by

$$S_G = 3000/\rho r \ (\mathrm{m}^2/\mathrm{g})$$

where $\rho = 2.2$ or 3.2 g/cm^3 and r = the particle radius, in nanometers. The accessible or measurable surface area using N_2 adsorption is somewhat lower than this amount due to the points of contact between the primary particles. This relationship is approximated by[8]

$$S = S_G(1 - na(2r + a)/4r^2) \ (\mathrm{m}^2/\mathrm{g})$$

where n = number of contacts per particle (coordination number), r = the particle radius, in nanometers, and a = 0.177 nm, the radius of a nitrogen molecule. The relationship between different packing types, their coordination numbers, and the resultant porosities ($\epsilon = \rho V_{pore}/[1 + \rho V_{pore}]$) is well established.[3,4,21] Thus, the pore volume and surface area as a function of coordination number and particle size can be determined. Alternatively, as shown in Tables 5 and 6, the coordination number and particle size can be calculated from the measured surface area and pore volume. Both the silica and alumina samples (except the silica sol dried without prior gelation) have calculated particle coordination numbers between four and five. More noteworthy is the fact that major discrepancies between the calculated and manufacturer's nominal particle sizes exist for all of the aluminas as well as the silica powders derived from the Nyacol 830 and 9950 sols. The calculated diameter for the Nyacol 830 sol is approximately a factor of 2 too large, while the calculated diameter for the Nyacol 9950 sol is about a factor of 3 too small. For the aluminas, the calculated spherical particle sizes are more similar to the crystallite sizes in the precursor sols (Table 2) than with the nominal particle size. For both the silica and alumina powders, the calculated particle sizes and the measured pore diameters ($2R_{pore,avg}$) are very similar.

It should be recognized that crystalline alumina is known to form cylindrical shaped fibers[23] or platelike

(21) Avery, R. G.; Ramsay, J. D. F. *J. Colloid Interface Sci.* **1973**, *42*, 597.

(22) Wefers, K.; Misra, C. *Oxides and Hydroxides of Aluminum*; Alcoa Laboratories, 1987.

(23) Trimm, D. L.; Stanislaus, A. *Appl. Catal.* **1986**, *21*, 215.

Table 7. Measured Particle Size Distributions of Silica Sol Precursors

Nyacol grade	manufacturer's nominal diam	vol-weighted Gaussian distribution particle diam	vol-weighted NICOMP distribution particle diam(s)
830	8 nm	12.5 nm	**14.4 nm** (93.51 vol %)
		$\chi^2 = 7.2$	45.0 nm (6.49 vol %)
2040	20 nm	11.2 nm	5.4 nm (55.04 vol %)
		$\chi^2 = 10.8$	**17.8 nm** (44.40 vol %)
			70.8 nm (0.56 vol %)
2034DI	20 nm	**21.2 nm**	26.4 nm (95.50 vol %)
		$\chi^2 = 1.9$	79.5 nm (4.50 vol %)
9950	100 nm	65.1 nm	**48.6 nm** (100 vol %)
		$\chi^2 = 8.5$	

structures,[22] and thus a spherical particle packing model may be of limited use for the alumina powders. A potential model of the geometrical surface area (the maximum area disregarding losses due to points of contact) for cylindrically shaped particles would be[23]

$$S_G = \frac{2000}{\rho}\left(\frac{1}{r} + \frac{1}{h}\right) (m^2/g)$$

where ρ is the density of the particle (g/cm^3), r is the radius of the base (nm), and h is the height of the cylinder (nm). However, determining appropriate values for r and h would be difficult, even with the use of a TEM or other such imaging method. If we instead use the manufacturer's crystallite sizes for the alumina sols in this cylindrical packing model, we find that the calculated values for S_G are, on average, 50% too high. This would indicate that there is a significant amount of surface area lost due to the points of contact between cylinders. This result is understandable if, for instance, there is some degree of uniaxial order among the cylinders. The contact area in this case would be large, resulting in a much lower measurable surface area. A model for platelike particles gives comparable results—calculated values for S_G overestimate the surface area, but the stacking of such particles would account for the difference between the calculated and measured surface areas. Thus, regardless of the choice of geometrical model (cylinders versus plates), we have additional evidence that the appropriate primary particle for an alumina gel is the crystallite size from the precursor sol.

In an effort to rectify the discrepancies between the calculated and nominal particle sizes for both the silica and alumina powders, the particle size distributions in the precursor sols were measured. Table 7 summarizes the particle size distribution data for the four silica sols, while Figure 2 shows the details of the volume-weighted particle size distributions. Table 8 and Figure 3 contain the corresponding data for the alumina sols. For all except the Nyacol 2034DI silica sol, the measured particle size distributions deviated significantly from the nominal particle sizes claimed by the manufacturer. In addition, as evidenced by the χ^2 values, the Nyacol 2034DI was seemingly the only sol that was sufficiently monodisperse for the Gaussian model of the particle size distribution to be appropriate. Among the silica sols, the Nyacol 830 and 9950 sols both have skewed distributions, while the Nyacol 2040 has essentially a bimodal distribution. For the alumina sols, the Dispal 23N4−20 and 18N4−20 are skewed to lower particle sizes, with the 18N4−20 sol being essentially trimodal. The Dispal 11N7−12 sol particle size distribution is skewed to larger particle sizes. Obviously, making assumptions about the particle size distributions in these commercial sols without any experimental verification could lead to erroneous conclusions.

As a demonstration of the usefulness of such data, Figure 4 shows the effect of the SiO_2 sol size on the measured surface area and pore volume of the powders prepared at low pH after calcination at 773 K for 2 h. These experimental results are compared to the theoretical spherical particle packing model. In Figure 4, note that *the particle diameters from the dynamic light-scattering experiments are used, not the nominal size given by the manufacturer*. For the surface area versus particle size plot, a coordination number of five was chosen as being representative for the calculated curve. The measurable surface area is a weak function of coordination number in the range of four to six except at very small (<10 nm) particle diameters and thus would have little effect on the shape of the calculated curve in the region of interest. Figure 4 shows that in the case of the powders prepared using the low pH preparation method with the base stable sols (Nyacol 830, 2040, and 9950), there is excellent agreement with the results of the spherical particle packing model provided the *correct* particle size data are used. In the case of the Nyacol 2040, the 17.8 nm size fraction, which accounts for 44.4 vol % of the sol, determines the structure of the final gel. Since the volume ratio of 17.8−5.4 nm diameter spherical particles is 35.8:1, the smaller particles are apparently filling in gaps between the larger particles without affecting the surface area and pore volume of the latter's structure. The powders prepared using the acid stable Nyacol 2034DI have surface areas 40% higher than predicted by the model but have calculated coordination numbers very similar to the other samples prepared in the same manner. There could be a large population of particles <5 nm not detectable by light scattering that are adding to the surface area but not affecting the pore volume. Alternatively, the primary particles in this sol could be very nonspherical, thus invalidating both the assumptions of the dynamic light-scattering method and of the particle packing model. This adds further complexity to explaining powders prepared from the Nyacol 2034DI silica sol considering that it was the only sol studied that was found to have a Gaussian particle size distribution.

The net result is that the silica powders prepared from the Nyacol 2034DI behave as if their primary particle diameter is closer to 15 nm rather than the measured 21.2 nm; in fact, its behavior is more similar to the Nyacol 830 than the Nyacol 2040 which would be expected from the manufacturer's nominal particle sizes. This assessment agrees with the fact that the pore size distribution plot (Figure 1) also showed that the Nyacol 2034DI behaved more like the Nyacol 830 than to the Nyacol 2040. An inappropriate comparison between the acid- and base-stable silica sols at the same nominal particle size (20 nm) would have been made without the experimentally determined particle size distributions.

The particle size distributions of the alumina sols can be explained in light of the evidence that the alumina crystallites are the source of the surface area and pore

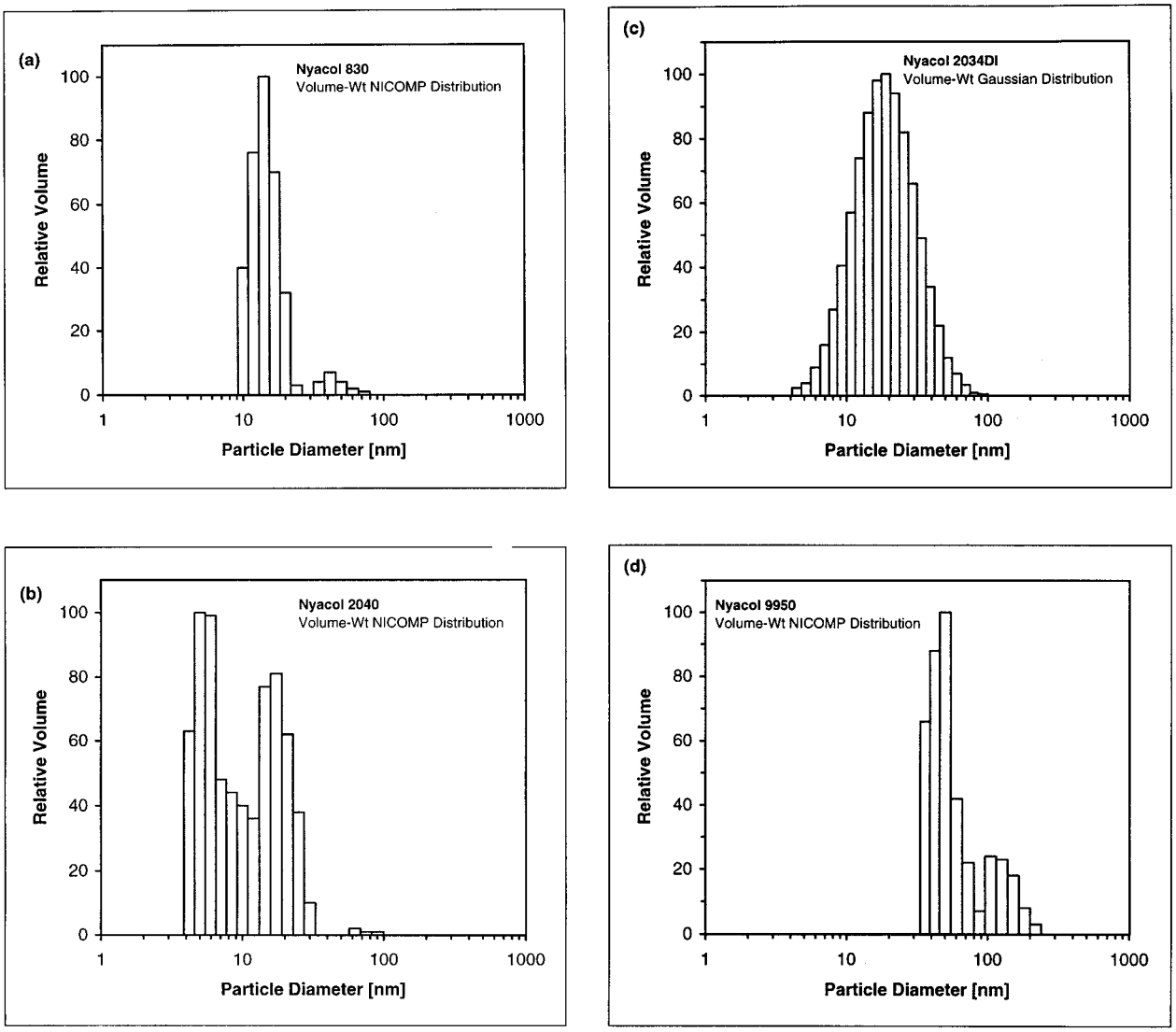

Figure 2. Volume-weighted particle size distributions of Nyacol grade (a) 830, (b) 2040, (c) 2034DI, and (d) 9950 colloidal silicas. Analysis performed by Particle Sizing Systems, Inc. on a NICOMP 370 submicron particle sizer.

Table 8. Measured Particle Size Distributions of Alumina Sol Precursors

Dispal grade	manufacturer's nominal diam	vol-weighted Gaussian distribution particle diam	vol-weighted NICOMP distribution particle diam(s)
11N7−12	415 nm	469.0 nm	191.1 nm (17.27 vol %)
		$\chi^2 = 13.4$	849.3 nm (82.72 vol %)
18N4−20	94 nm	55.7 nm	17.4 nm (59.65 vol %)
		$\chi^2 = 26.6$	60.1 nm (36.58 vol %)
			212.4 nm (3.77 vol %)
23N4−20	90 nm	31.3 nm	13.3 nm (77.06 vol %)
		$\chi^2 = 16.9$	52.5 nm (21.61 vol %)
			372.0 nm (1.33 vol %)

volume in the alumina powders. The fact that the Dispal 23N4−20 and 18N4−20 are skewed to smaller particle sizes could mean that there is some breakdown of the sol particles into smaller aggregates of their component crystallites over time, even if the manufacturer's nominal sizes were initially accurate. The much larger initial aggregate and crystallite size of the Dispal 11N7−12 may help it to resist this breakdown into smaller particles, and thus the process is not so pronounced in that case. The preparation method used by Vista which results in the different sol sizes also seems to cause their internal structure to be different—the boehmite crystallite size in the precursor sols seems to increase with increasing sol size. If the boehmite crystallite size could be controlled independent of particle size, it would then be possible to prepare alumina powders that are texturally identical from precursor sols of different sizes. While the internal structure of the alumina sols is different from that of the silica sols (porous vs nonporous), in both cases there is a fundamental physical structure which can be used to explain their textural properties.

Effect of Precursor Sol Size on DRIFT Spectra. Figure 5 shows the in situ DRIFT spectra at 473 K for silica powders derived from the Nyacol 830, 2040, and 9950 silica sols. The powders were all prepared at low pH with a composition of 3.5 M SiO_2 and 6.5 M HNO_3 and subsequently heat treated to 773 K. Also included for comparison is a spectrum from a silica aerogel made from tetraethyl orthosilicate (TEOS) and heat treated to 773 K. Applying the spherical particle packing model to the TEOS aerogel (785 m^2/g surface area, 2.59 cm^3/g pore volume) yields a calculated particle diameter of 3.0 nm and a particle coordination number of 2.3. These values are reasonable considering current models for the structure of silica aerogels.[8,15] In the hydroxyl region, the isolated silanol ($\nu = 3750$ cm^{-1}) peak is the most

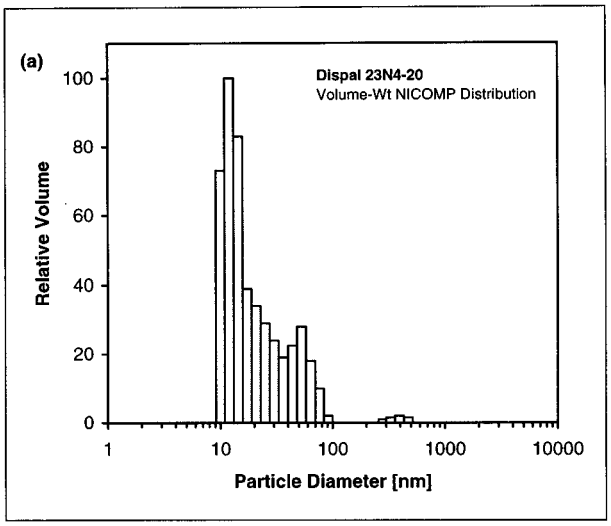

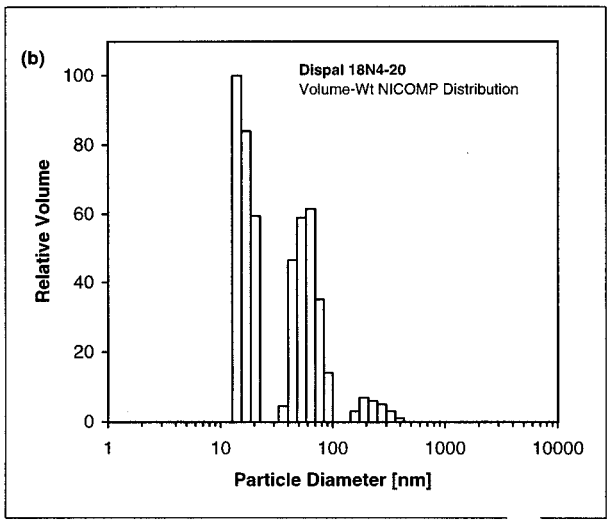

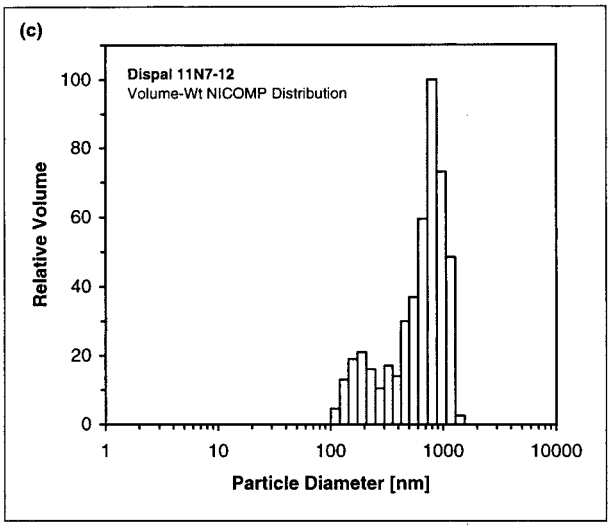

Figure 3. Volume-weighted particle size distributions of Dispal grade (a) 23N4−20, (b) 18N4−20, and (c) 11N7−12 colloidal aluminas. Analysis performed by Particle Sizing Systems, Inc. on a NICOMP 370 submicron particle sizer.

intense in the TEOS aerogel and the least intense in the Nyacol 9950 powder, with the Nyacol 2040 and 830 powders having approximately equal intensities. Since the Nyacol 2040 and 830 sols had approximately the same particle size according to the dynamic light-

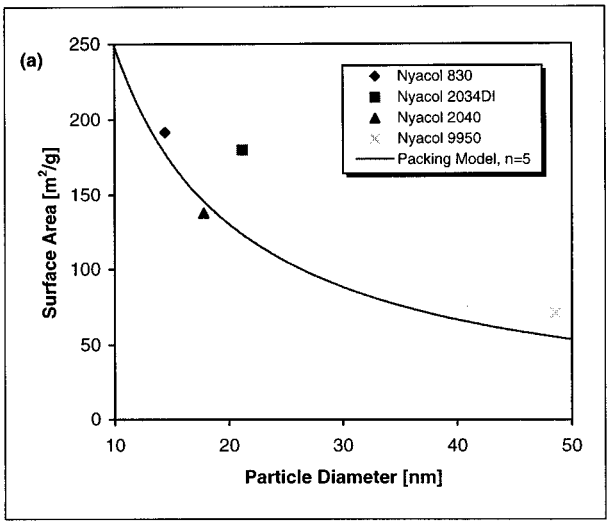

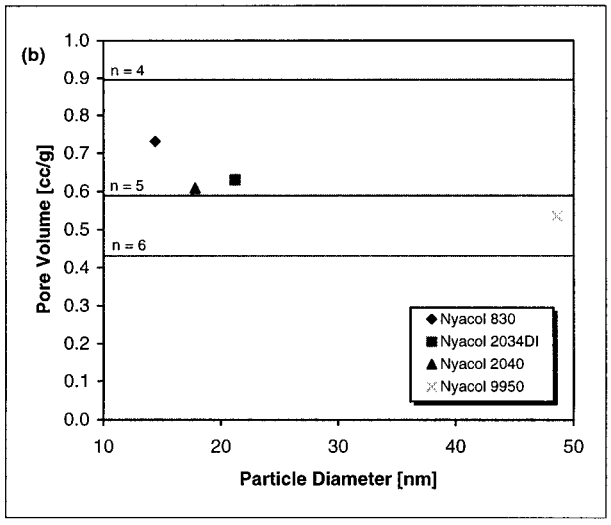

Figure 4. Effect of sol size on (a) surface area and (b) pore volume of silica powders. Gels prepared at low pH with composition of 3.5 M SiO_2 and 6.5 M HNO_3. Powders calcined at 773 K for 2 h.

scattering experiments, we can conclude that the number of isolated silanol groups per unit sample volume is inversely proportional to the primary particle size.

A second effect of particle size can be seen in the broad 900−1300 cm^{-1} peak in the structural region. This peak is in fact made up of three separate features: (1) ∼960 cm^{-1} (Si−OH stretch), (2) ∼1080 cm^{-1} (TO or transverse mode of asymmetric Si−O−Si stretch), and (3) ∼1220 cm^{-1} (LO or longitudinal mode of asymmetric Si−O−Si stretch).[15,24,25] The raw data plotted in Figure 5a seem to show a trend toward higher wavenumber with larger particle size. The data were then deconvoluted using Jandel Scientific's PeakFit software (v. 3.00). Spectral data from 875 to 1400 cm^{-1} were fit using three Gaussian peaks and a linear baseline. The results for the asymmetric peaks are plotted in Figure 6. Figure 6 also includes results for the corresponding powder from the Nyacol 2034DI sol. Increasing particle size leads to an increase in both asymmetric frequencies, with the exception of the Nyacol 2034DI powder. Much

(24) Duran, A.; Serna, C.; Fornes, V.; Fernandez Navarro, J. M. *J. Non-Cryst. Solids* **1986**, *82*, 69.
(25) Ying, J. Y.; Benziger, J. B. *J. Am. Ceram. Soc.* **1993**, *76*, 2561.

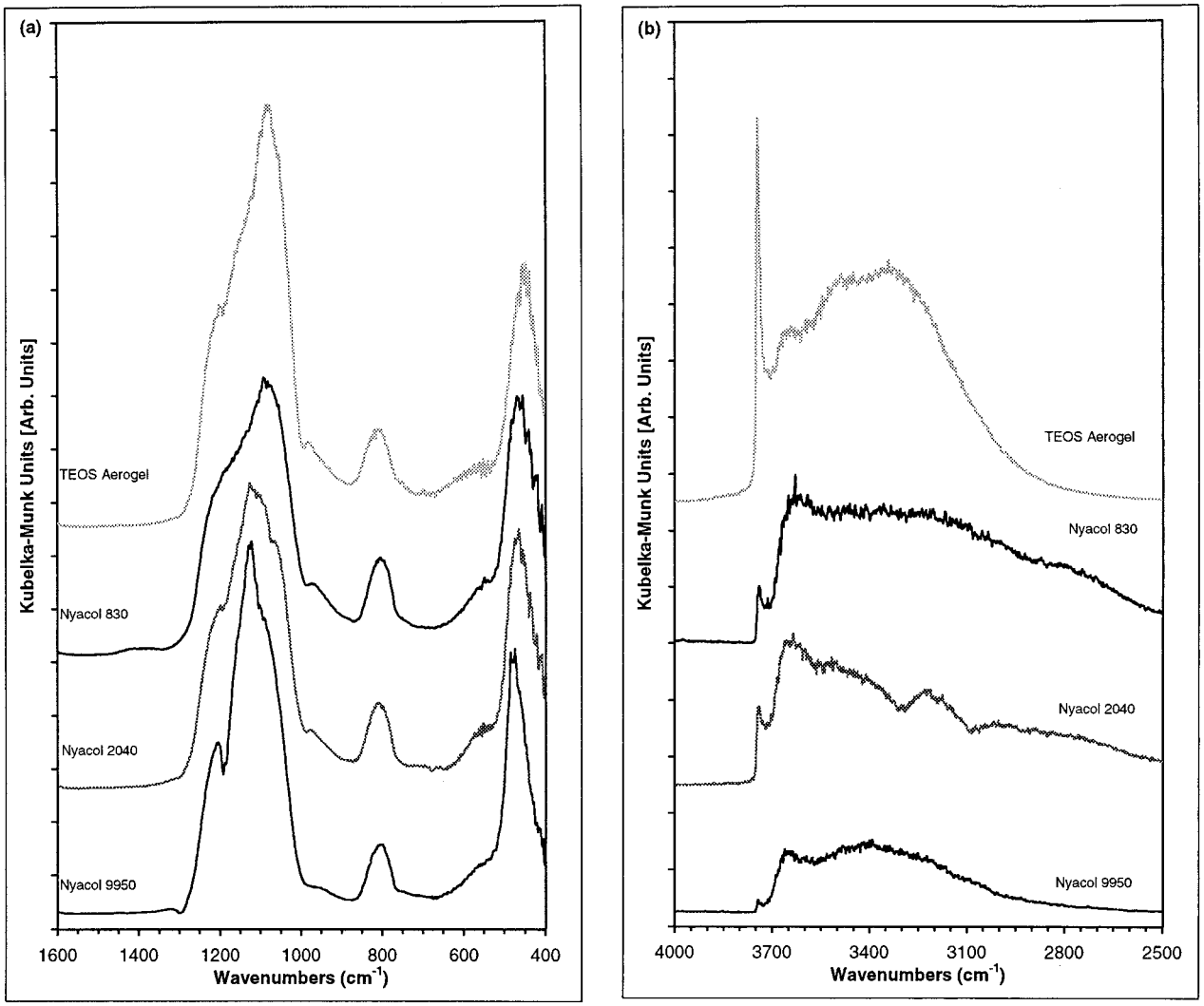

Figure 5. Effect of precursor sol size on silica in situ DRIFT spectra: (a) structural region at 473 K and (b) hydroxyl region at 473 K. Nyacol gels prepared at low pH with composition of 3.5 M SiO_2 and 6.5 M HNO_3. All powders calcined at 773 K for 2 h. Scans taken after 50 min with He flow at 50 cm^3/min.

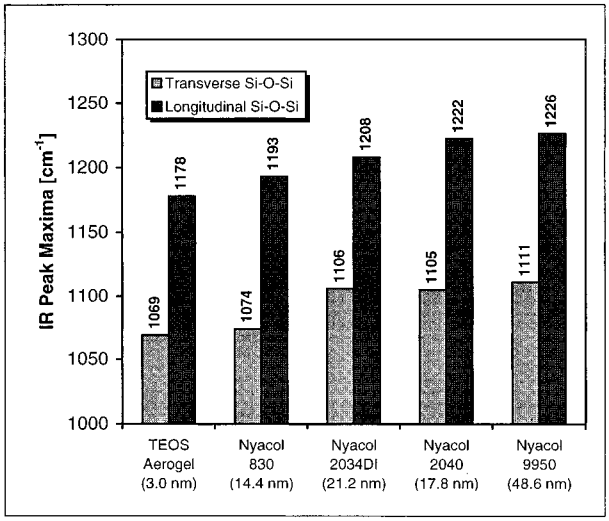

Figure 6. Effect on Si−O−Si bond stretch frequencies of silica precursor particle size. Nyacol gels prepared at low pH with composition of 3.5 M SiO_2 and 6.5 M HNO_3. All powders calcined at 773 K for 2 h. In situ scans taken at 473 K after 50 min. He flow at 50 cm^3/min DRIFT spectra deconvoluted with PeakFit software to determine frequency location.

as it did with the textural properties, the Nyacol 2034DI powder behaves as if its primary particle diameter is closer to 15 nm rather than the DLS-measured 21.2 nm. This is further evidence that there might be a population of small particles not detected by light scattering or that the primary particles in this acid-stable silica sol are very nonspherical. It is known that the asymmetric frequencies are sensitive to the strength of the silica network. As noted by Brinker and Scherer, increases in the frequencies of the asymmetric Si−O−Si stretching vibrations with increasing heat treatment in alkoxy-derived aerogels can be related to a strengthening of the silica network through cross-linking.[15] Duran et al. observed a shift from 1080 to 1150 cm^{-1} in TEOS xerogels, which they attributed to the strengthening of a silica network as it sinters.[24] Miller et al. found that in titania−silica aerogels, decreases in the frequencies of these vibrations with increasing titania content could be attributed to the weakening of the silica network by the presence of the titania.[26] Extending the model of the silica gels used in the spherical particle packing model, the silica network of the silica powders being studied can now be envisioned as marbles of a fixed size connected to four to five other marbles with sticks. These marbles are nonporous and are composed of a densely cross-linked network of silica, i.e., a strong

(26) Miller, J. B.; Johnston, S. T.; Ko, E. I. *J. Catal.* **1994**, *150*, 311.

internal network. With small particles, the relative proportion of interparticle bonds ("sticks") compared to the total number of Si−O−Si bonds is higher than that of powders with larger primary particles, and thus the cross-linking density in the overall network is lower. A powder with a small primary particle size can then be envisioned as having a weaker silica network than a powder with larger particles. Since the IR stretch frequencies can be considered average properties of the bulk powder, within this framework the correlation of the stretching vibrations with particle size can now be understood.

Ex situ DRIFT spectra of the 1.0 M Al_2O_3/0.0 M HNO_3 subset of alumina powders calcined to 773 K show very little difference in their structural regions. All show a characteristic "double-hump" which can be associated with the γ transitional crystalline phase of alumina.[22] The hydroxyl regions of these spectra show no distinct features in either ex situ or in situ DRIFT experiments, indicating a lack of isolated hydroxyl groups. The integrated area under this hydroxyl peak does decrease with increasing particle size, but this is likely merely an effect of the corresponding reduction in surface area.

Effect of Preparation Method. As described in the Experimental Section, a number of general preparation techniques were utilized to prepare both the silica and alumina powders. As shown in Table 3, all four techniques used with the silicas were applied to the Nyacol 830 sol. The low pH preparation method followed by the ethanol wash produced powders with the highest surface areas and pore volumes after calcination at 773 K (Table 5), with the sample prepared at low pH but without the ethanol wash a close second. In the case of the vacuum-dried sol sample, the pore volume after calcination to 773 K corresponds to a particle coordination number of 8.6, versus 4.0 and 4.4 for the powders prepared at low pH. The advantage of first producing a gel before drying is evident by comparing the porosity of 36% for the dried sol versus 66% and 62% for the low pH gels. One possible explanation is that the formation of siloxane bonds between particles before drying the wet gel helps to stabilize it and allows for a much less dense gel after drying and calcination. Once the siloxane bonds are formed, they are difficult to break and thus resist the capillary forces present in the pores during drying. The powder made by simple drying was able to pack much more efficiently because these interparticle bonds were not formed until the drying step. A much higher coordination number results because the particles are able to rearrange easily while the solvent is being removed. The corresponding decrease in surface area is a result of this much tighter packing.

The final preparation technique used with the Nyacol 830 sol was the preparation with 1-propanol. The technique formed a very light, dispersible powder, but the measured surface area and pore volume were in fact lower than that of the low-pH powders after calcination at 773 K. After drying at 383 K, these samples all had surface areas of ~200 m^2/g, but the 1-propanol gel had the lowest pore volume of the three (0.72 vs 0.91 and 0.86 cm^3/g). The Nyacol 2034DI powders prepared at low pH and with 1-propanol gave similar results. These observations all suggest that the low-pH wet gels have the strongest interparticle bonds and thus are affected less by capillary forces during drying. The presence of the alcohol in the pores should have resulted in lower capillary forces than water during drying,[8] and thus this loss of textural properties with heat treatment was unexpected. If the drying forces were less for the 1-propanol gels and yet they still sintered at a lower temperature, the interparticle bonds prior to drying must have been weaker. In a model of the interparticle bonding in the samples before drying, an ungelled sol would have only hydrogen bonding between the particles, while the low-pH powders would have mainly covalent siloxane bridges between the particles. The 1-propanol gels would then seem to have some mixture of the two types of bonding, resulting in a gel network of intermediate strength. In the ethanol-washed, low-pH powder prepared from the Nyacol 830 sol, the high surface area and pore volume are a result of the benefits of forming the strong interparticle network at low pH coupled with the lowering of capillary forces during drying due to the solvent exchange of the alcohol for water.

The effects of changing the silica and acid concentration in the wet gels were also explored. The concentration of silica and acid were varied in powders prepared from the Nyacol 2040 colloidal silica using the low-pH preparation method. Table 5 lists the measured BET surface areas and pore volumes of these four powders after calcination at 773 K. For this precursor, the surface area, pore volume, and pore size distributions after calcination at 773 K were almost identical despite the changes in the silica and acid concentration in the wet gel. The mean surface area of these four powders was 148 m^2/g, with a standard deviation of 8.5 m^2/g, or 5.7% of the mean. Also listed in Table 3 is a pair of powders prepared from the Nyacol 2034DI colloidal silica, which led to similar results. *The textural properties of the powders are determined solely by the initial sol size distribution and not on the silica or acid concentrations in the wet gel.* This observation verifies statements made by Iler that gels made from particles of a given size dry to the same final area and pore volume regardless of the wet gel silica concentration.[8] This is true only within a given preparation method, as evidenced by the differences in the samples prepared from the Nyacol 830 compared previously. The only effect of changing the silica and acid concentration was the gel time—lowering the concentration of silica or nitric acid led to increased gel times. In fact, the two effects appear to be additive. Lowering the silica concentration from 3.5 to 2.5 M at constant nitric acid concentration led to a 2.8-fold increase in gel time. Lowering the acid concentration from 6.5 to 4.5 M at constant silica concentration led to an 11-fold increase in gel time. Changing both simultaneously, for example from 3.5 M SiO_2 and 6.5 M HNO_3 to 2.5 M SiO_2 and 4.5 M HNO_3, increased the gel time by a factor of 32, or the product of the two effects. One can thus change these two parameters independently to control gel time.

As described in the Experimental Section, three general preparation techniques were used with the alumina sols: drying the precursor sol without first forming a gel, preparing a gel by the addition of nitric acid, and preparing a gel by addition of ammonium hydroxide. Within the nitric acid preparation method,

powders were prepared from the Dispal 23N4−20 and 18N4−20 alumina sols which covered a range of alumina and acid concentrations. The addition of any acid at all resulted in a slightly lower surface area compared to drying without first forming a gel, but these differences were minor. The addition of the acid may be helping to break up the initial boehmite sol particles or peptize some of the alumina, which could then pack more tightly in the wet gel and subsequently dried sample. However, the corresponding pore size distribution data show little difference between the powders prepared from the same precursor by drying or with acid. The Dispal 23N4−20 powder prepared with ammonium hydroxide had a surface area after calcination at 773 K much like that of the other two preparation methods. The only textural difference found was a slightly higher pore volume and a pore size distribution correspondingly shifted to larger pores. The boehmite transformation into γ-Al_2O_3 between 523 and 773 K apparently causes sufficient rearrangement of the microstructure of the powders to essentially mask any preparation effects in these alumina powders. While we were able to manipulate the textural properties of the silica powders by using different preparation techniques, the level of textural control achievable with the alumina sols via preparation seems to be much less. This is a direct consequence of the precursor alumina sols being composed of crystallites of alumina as opposed to being nonporous spheres as was the case for the silica sols.

Effect of Heat Treatment. The effect of heat treatment on the textural properties of the silica and alumina powders was also investigated. Up to six different heat treatment points were examined: after 383 K vacuum-drying, after 523 K vacuum-drying, after 773 K calcination, after 1173 K calcination, after 1373 K calcination, and after 1473 K calcination. Each heat treatment was performed on portions of the powders which had been previously dried or calcined to the prior temperature. Changes in the surface area and pore volume with heat treatment are shown in Figure 7 for silica powders prepared at low pH with gel compositions of 3.5 M SiO_2 and 6.5 M HNO_3. Powders from all four silica sols were prepared using this composition, facilitating comparisons between the silica sol precursors. At temperatures up to and including 773 K, surface areas remained constant for all of the powders. At 1173 K the surface areas and pore volumes of powders gelled from the Nyacol 830 and 2040 dropped to essentially zero, while that gelled from the Nyacol 2034DI retained 91% of its 773 K surface area and 89% of its 773 K pore volume. At 1173 K the Nyacol 9950 powder retained 76% of its 773 K surface area and 91% if its 773 K pore volume. Even at 1373 K the Nyacol 2034DI powder still retained 43% and 41% of its 773 K surface area and pore volume, respectively, while the Nyacol 9950 powder dropped to zero.

A combination of particle size and impurity effects can explain the differences between the powders prepared from the Nyacol 830 and 2040 versus the 2034DI and 9950 silica sols. The rate of densification is inversely proportional to particle radius,[15,27] and alkali impurities are known to lower sintering temperatures in silica gels.[8,28] Powders derived from the Nyacol 2034DI and 9950 sols are thus more likely to resist surface area and pore volume losses during heat treatment. XRD and ex situ DRIFT studies of these powders show that the Nyacol 830 and 2040 had crystallized to cristobalite after calcination at 1173 K, indicating that the catastrophic loss of surface area and porosity was accompanied by this crystallization. Crystallization is delayed in the Nyacol 9950 powder until 1373 K, while the Nyacol 2034DI powder is only partially crystalline at 1373 K. As shown in Tables 1 and 7, the Nyacol 9950 had both the largest size particles as well as the lowest initial sodium concentration of the base-stable sols, while Nyacol 2034DI contains no Na_2O. These examples show the significant role that impurities and particle size can have on the sintering and crystallization behavior of silica.

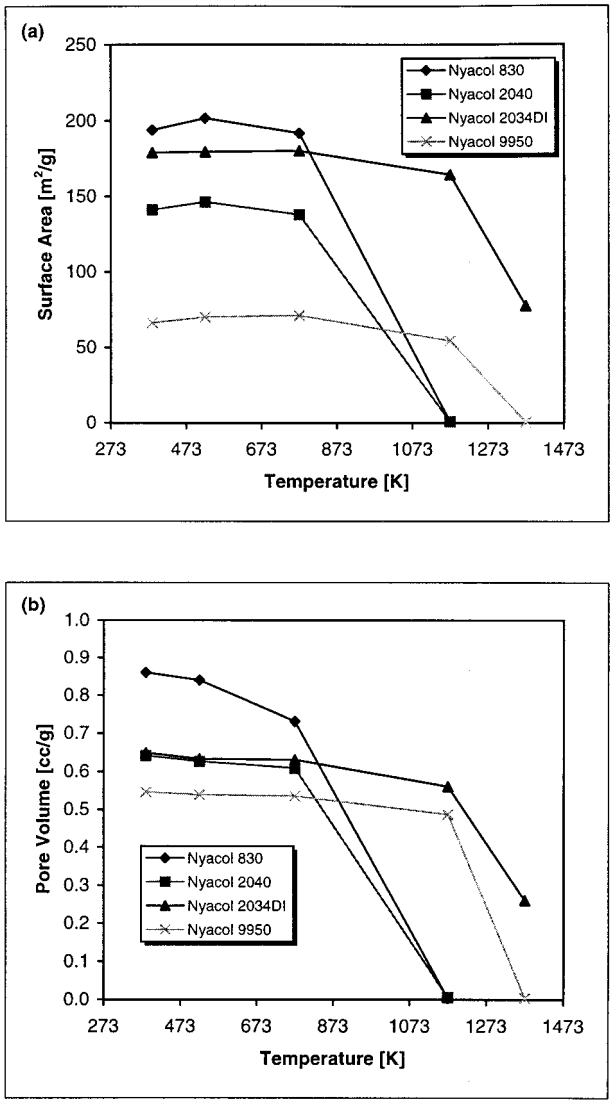

Figure 7. Effect of heat treatment on (a) surface area and (b) pore volume of silica powders. Gels prepared at low pH with composition of 3.5 M SiO_2 and 6.5 M HNO_3.

Figure 8 shows the corresponding data for the Nyacol 830 powders prepared using the four different preparation techniques described previously. At 1173 K, all four samples sintered to very low surface areas and crystal-

(27) Frenkel, J. *J. Phys. (Moscow)* **1945**, *9*, 385.

(28) Ries, H. E., Jr. In *Advances in Catalysis and Related Subjects*; Academic Press: New York, 1952; Vol. 4.

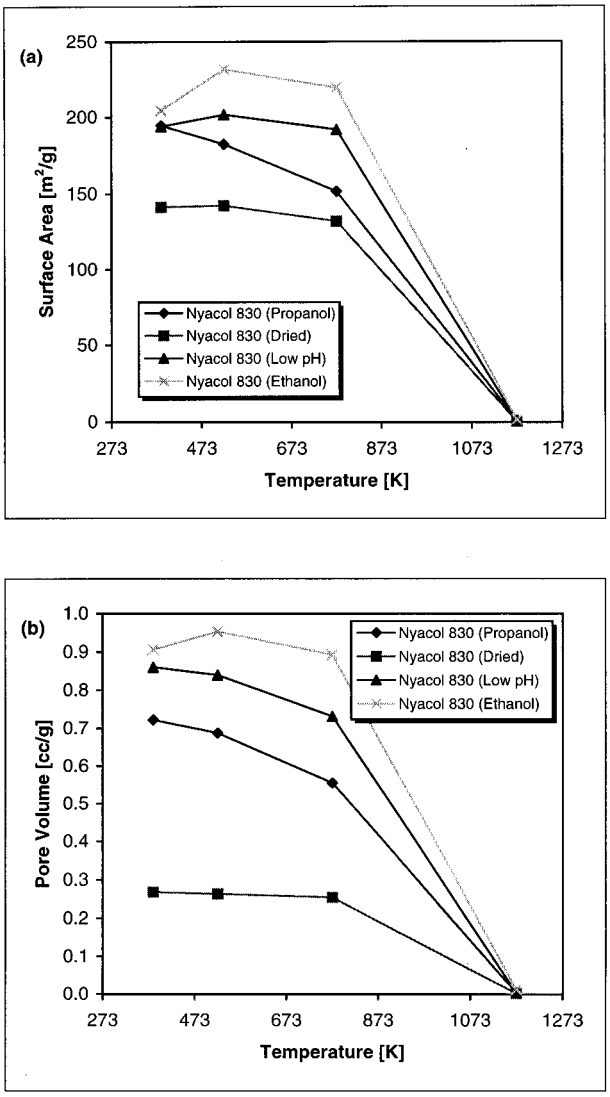

Figure 8. Effect of heat treatment on (a) surface area and (b) pore volume of Nyacol 830 silica powders prepared using 1-propanol, low pH, low pH + ethanol wash, and ungelled drying techniques.

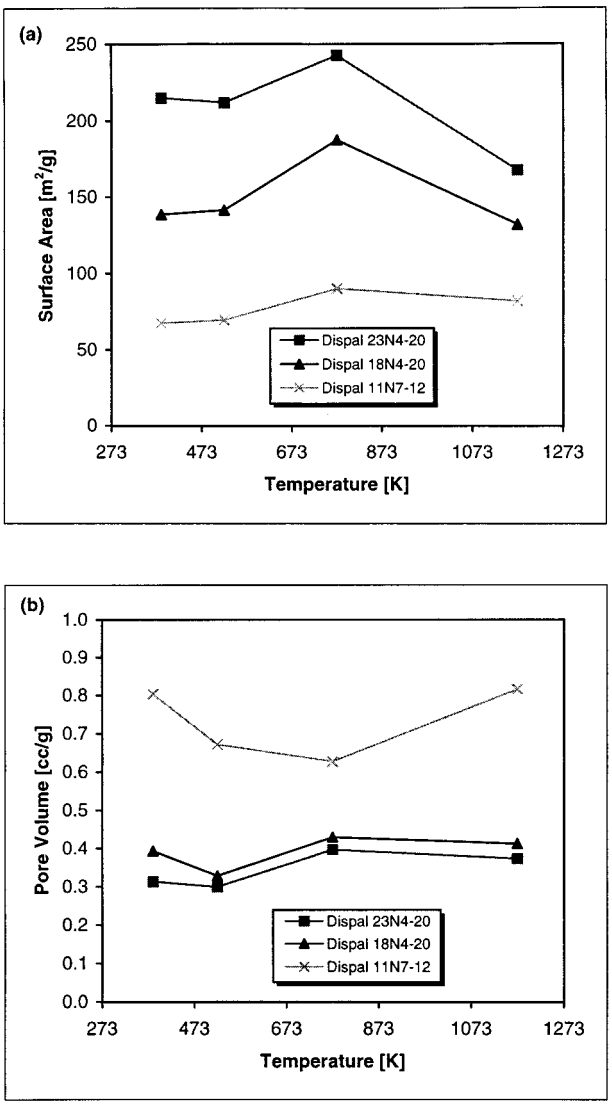

Figure 9. Effect of sol size and heat treatment on (a) surface area and (b) pore volume of alumina powders. Powders prepared by vacuum-drying with a composition of 1.0 M Al_2O_3 and 0.0 M HNO_3.

lized into cristobalite. At all other temperatures, the low pH plus ethanol wash preparation technique led to a powder with the highest surface area and pore volume, while the ungelled, dried sol method had the lowest surface area and pore volume. The thermal stability of the ungelled sol powder until the point that it loses surface area rapidly can be attributed to its close particle packing once it was dried. Forming the powder by drying the sol without prior gelation allows the particles to rearrange during the drying process, but once they have packed tightly the mobility of the particles is inhibited during further heat treatment. The powders prepared at low pH exhibit surface area stability similar to the ungelled sol powder with a maximum in surface area at 383 K, while their pore volumes begin to drop between 383 and 773 K. Apparently there is some slight rearrangement of the particles in the powder during the heat treatment which results in pore shrinkage without a significant change in the surface area. Using the spherical particle packing model with a constant particle size of 13.3 nm, changing the particle coordination number from 4.1 (at 383 K) to 4.4 (at 773 K) can account for this change in pore volume in the powder prepared at low pH without the ethanol wash. Both the measured surface area and pore volume of the powder prepared with 1-propanol drop over the course of heat treatment, providing further evidence that the 1-propanol preparation technique results in a wet gel with a weaker overall structure than the low pH method.

Changes in the surface area and pore volume with heat treatment are shown in Figure 9 for aluminas prepared with compositions of 1.0 M Al_2O_3 and 0.0 M HNO_3. At the first two heat-treatment temperatures (383 and 523 K), the surface area of all three powders remains constant while the pore volumes drop slightly. This drop is likely caused by the removal of water from within the alumina framework. The surface areas go through a maxima at 773 K and then begin to drop at 1173 K. The pore volumes for the Dispal 23N4−20 and 18N4−20 increase slightly at 773 K and remain essentially constant to 1173 K, while the Dispal 11N7−12 goes through a minima at 773 K. These results are consistent with the findings of other researchers. For example, Wefers and Misra stated that "if the calcination temperature is raised above 650−700 K, the surface

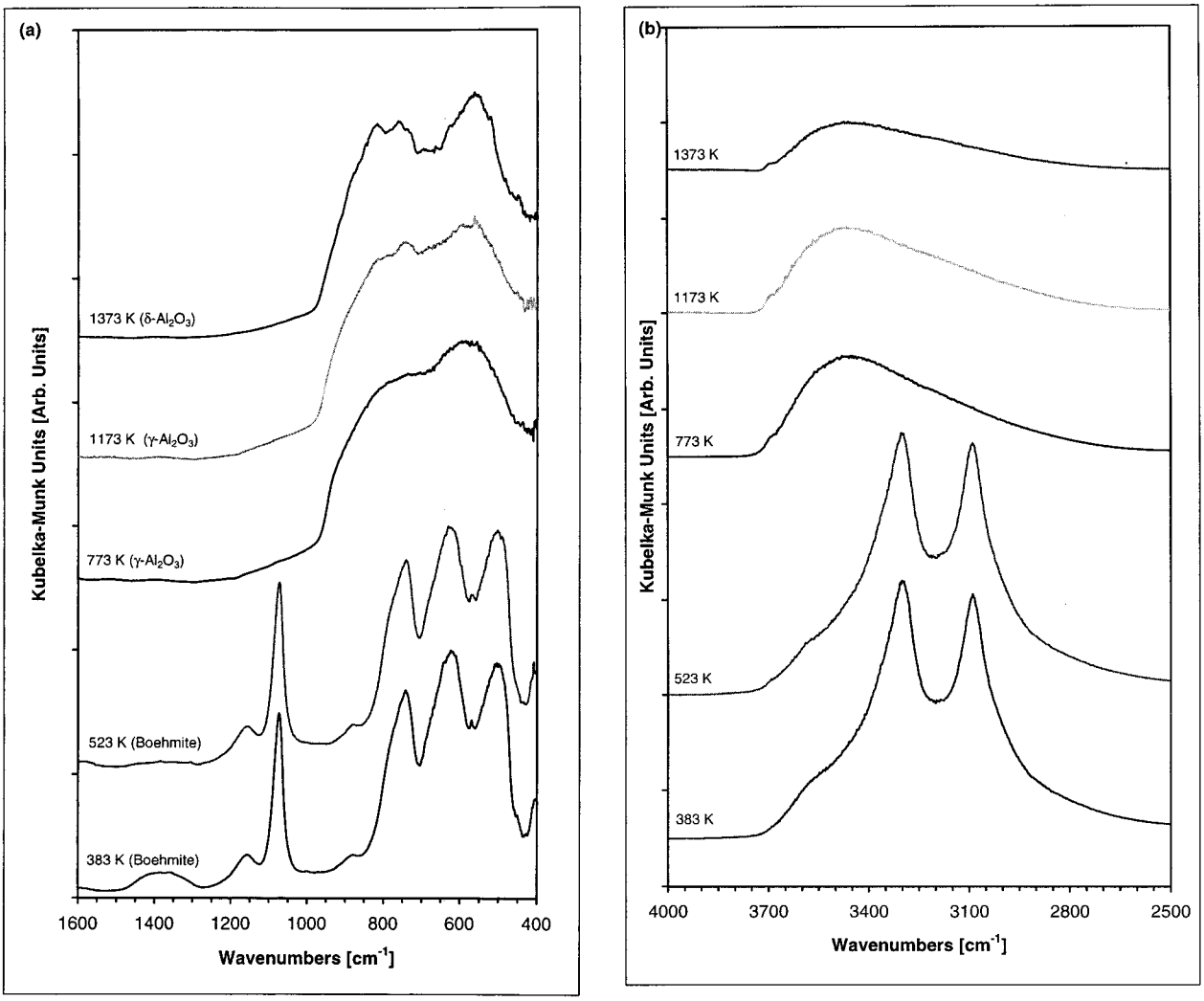

Figure 10. Effect of heat treatment on ex situ DRIFT spectra of alumina powder prepared from Dispal 18N4−20 with a gel composition of 1.5 M Al_2O_3 and 0.14 M HNO_3: (a) structural region and (b) hydroxyl region.

area diminishes but the pore volume increases slightly".[22] In this process, the initially small crystallite domains of alumina coalesce into larger, more stable areas of oxide. The spacing between these domains also increases, which results in the larger pore volume accessible to nitrogen BET analysis.[22] This effect is countered by the dehydroxylation of the boehmite as it transforms to the transitional gamma alumina form. In the Dispal 23N4−20 and 18N4−20 powders, the coalescence effect is dominant since the initial crystallite size is small. In contrast, the dehydroxylation effect is dominant in the Dispal 11N7−12 powder since the crystallites in the Dispal 11N7−12 powder are large enough initially, resulting in the slight decrease in pore volume between the 423 and 773 K heat treatments. The pore size distributions for all three alumina sols show a corresponding shift toward larger pores with increasing heat treatment, consistent with the observations of Trimm and Stanislaus.[23]

Ex situ DRIFT spectra of the 1.5 M Al_2O_3/0.14 M HNO_3 powder prepared from the Dispal 18N4−20 alumina sol are shown in Figure 10. These plots show the structural transformations which these alumina sol derived materials undergo upon heat treatment and help to explain the changes in the textural properties described above. The ex situ DRIFT spectra of the other alumina powders undergo identical transformations. At 383 and 523 K, the DRIFT spectra show the characteristics of well-crystallized boehmite.[22] This comes as no surprise since, according to the manufacturer, the precursor sol is itself boehmite. At 773 K the DRIFT spectra undergoes a significant change, as the structural region (Figure 10a) becomes dominated by a broad "double hump" between 400 and 1000 cm^{-1}, while a broad hydroxyl peak replaces the twin boehmite −OH stretches at 3089 and 3302 cm^{-1} (Figure 10b). The structural peak becomes better resolved into its two (or more) subpeaks as the calcination temperature is increased to 1373 K. As shown in Figure 11, concurrent X-ray diffraction studies have shown that after calcination at 1173 K the powder is γ-Al_2O_3, while at 1373 K it is δ-Al_2O_3. At 1473 K, the 1.0 M Al_2O_3/0.14 M HNO_3 powder prepared from Dispal 23N4−20 has fully transformed into α-Al_2O_3 (corundum). This combination of IR and XRD data indicate that, not surprisingly, these sol-derived materials undergo a normal progression through the transitional phases of alumina when well-crystallized boehmite is the precursor: boehmite → gamma → delta → theta → alpha. We were unable to "capture" the theta transitional phase given the high-temperature heat treatments used in this study, but there is no reason to suspect that the phase would not be present under a more complete set of heat-treatment conditions. Murrell and Tauster[6] found their 2 and 20−

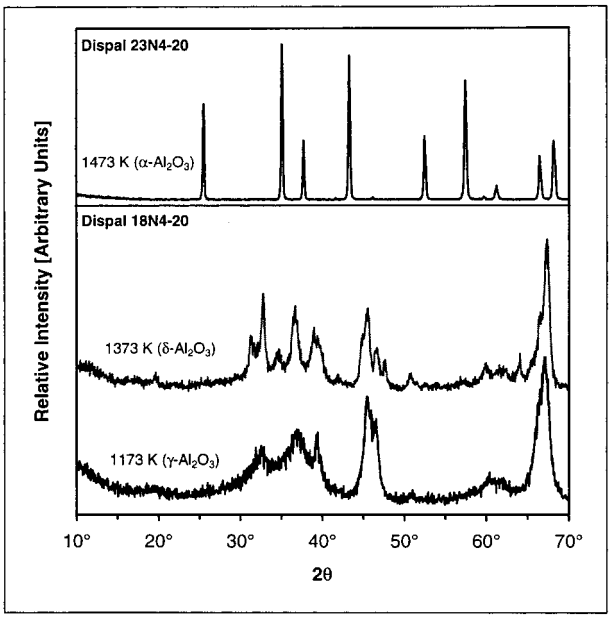

Figure 11. Effect of heat treatment on XRD spectra of alumina powder prepared from Dispal 23N4−20 (1.0 M Al_2O_3 and 0.14 M HNO_3) and Dispal 18N4−20 (1.5 M Al_2O_3 and 0.14 M HNO_3).

30 nm sols gelled with NH_4OH to be boehmite at 473 K but δ-Al_2O_3 at both 773 and 1173 K, indicating that their aluminas transform much earlier to the δ-Al_2O_3 transition phase than the alumina powders we have prepared (773 vs 1373 K). Despite this difference in the transitional phase behavior, the textural properties of Murrell and Tauster's alumina prepared from a 20−30 nm sol are very similar to the Dispal 23N4−20 powders prepared in this study. This would seem to indicate that the alumina sols in both studies have similar crystallite sizes, so the cause of this early transformation to δ-Al_2O_3 is unknown. The preparation and heat treatment procedures used in both studies were similar enough that it is unlikely that they could be the cause.

Acidic Properties Probed by Pyridine Adsorption. In situ pyridine adsorption experiments, following a stepwise adsorption protocol as described earlier, were performed on a number of the powders in this study. Estimations of the relative Lewis and Brønsted acid site populations were determined using the method of Basila and Kantner.[29] The calculations showed that, at all temperatures, the alumina powders contained only Lewis acid sites. There was no evidence of the Brønsted-only IR peak ($\nu \approx 1540$ cm^{-1}) in any of the spectra. The silica powders tested showed no evidence of any acid sites strong enough to adsorb pyridine within the range of temperatures studied. Some hydrogen-bonded pyridine was detected after the initial pyridine dose but was gone by the 423 K step in the procedure. This hydrogen-bonded pyridine was likely associated with the hydroxyl population of the silica surface, and such a weakly bound species would not be expected to remain at elevated temperatures. For the aluminas, calculation of the percent of the acid sites remaining versus temperature indicated that the alumina powders possessed acid sites that are similar in strength distribution. As shown in Figure 12, the preparation method and precursor sol size did not appear to affect the acid strength of the calcined aluminas.

(29) Basila, M. R.; Kantner, T. R. *J. Phys. Chem.* **1966**, *70*, 1681.

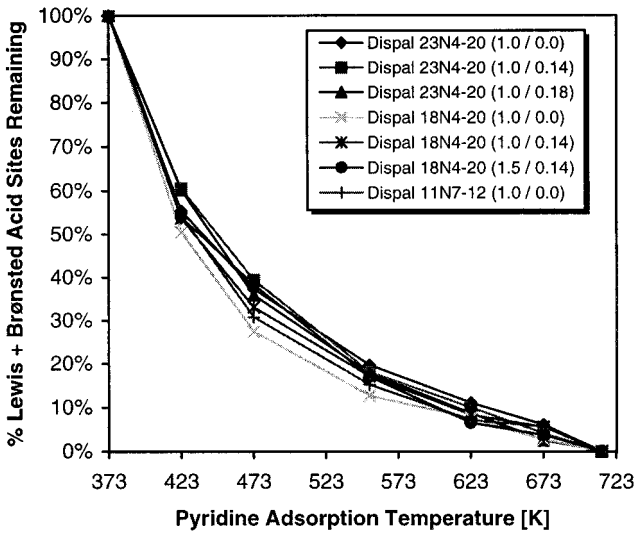

Figure 12. Effect of initial alumina gel composition on percentage of acid sites remaining with increasing temperature. Powders calcined at 773 K for 2 h. Data derived from in situ pyridine adsorption experiments.

Conclusions

The results of this study clearly establish the importance of characterizing commercially available preformed sols in understanding the properties of calcined powders prepared from them. Although the fundamental structures of the silica and alumina sol precursors studied were different, we have shown that the textural and chemical properties of their calcined oxides can be understood within the framing concept of a continuum of molecular-scale building blocks. Simple geometric particle packing models provide a useful aid in this understanding. The fact that preparation methods could be used to control the textural properties of the silicas but not the aluminas is directly related to the differences in the primary structural units of the alumina and silica sol precursors. This inherent complexity of using nonmodel precursors can thus be mitigated by the systematic exploration of such variables as precursor sol size and preparation method. This study, aimed at linking fundamental research and industrial application, provides a foundation for using commercially available sols in the preparation of single as well as multicomponent oxides.

Acknowledgment. We thank the National Science Foundation for supporting this work via Grant CTS-9522066 and a graduate fellowship for S.J.M. We also thank Eka Nobel, Inc., and Vista Chemical Co. for providing us with sol samples.

CM970271H